

Article

Robust Burst Detection Algorithm for Distributed Unique Word TDMA Signal

Kunheng Zou , Peng Sun , Jicai Deng *, Kexian Gong  and Zilong Liu 

School of Information Engineering, Zhengzhou University, 100 Science Avenue, Zhengzhou 450001, China; zoukunheng@gs.zzu.edu.cn (K.Z.); iepengsun@zzu.edu.cn (P.S.); kxgong@zzu.edu.cn (K.G.); zilongliu@gs.zzu.edu.cn (Z.L.)

* Correspondence: iejdeng@zzu.edu.cn

Abstract: In recent years, distributed unique word (DUW) has been widely used in satellite single carrier TDMA signals, such as very small aperture terminal (VSAT) satellite systems. Different from the centralized structure of traditional unique word, DUW is uniformly dispersed in a burst signal, where the traditional unique word detection methods are not applicable anymore. For this, we propose a robust burst detection algorithm based on DUW. Firstly, we allocated the sliding detection windows with the same structures as DUW in order to effectively detect it. Secondly, we adopt the method of time delay conjugate multiplication to eliminate the influence of frequency offset on detection performance. Due to the uniform dispersion of DUW, it naturally has two different kinds of time delays, namely the delay within the group and the delay between the two groups. So, we divide the traditional dual correlation formula into two parts to calculate them separately and obtain a dual correlation detection algorithm, which is suitable for DUW. Simulation and experimental results demonstrate that when the distribution structure of DUW changes, detection probability of the proposed algorithm fluctuates little, and its variance is 1.56×10^{-5} , which is 99.83% lower than the existing DUW detection algorithms. In addition, its signal to noise ratio (SNR) threshold is about 1 dB lower than the existing algorithms under the same circumstance of the missed detection probability.

Keywords: satellite communication; distributed unique word; TDMA; burst detection; robustness



Citation: Zou, K.; Sun, P.; Deng, J.; Gong, K.; Liu, Z. Robust Burst Detection Algorithm for Distributed Unique Word TDMA Signal. *Electronics* **2022**, *11*, 89. <https://doi.org/10.3390/electronics11010089>

Academic Editor: Cheonshik Kim

Received: 16 November 2021

Accepted: 25 December 2021

Published: 28 December 2021

Publisher's Note: MDPI stays neutral with regard to jurisdictional claims in published maps and institutional affiliations.



Copyright: © 2021 by the authors. Licensee MDPI, Basel, Switzerland. This article is an open access article distributed under the terms and conditions of the Creative Commons Attribution (CC BY) license (<https://creativecommons.org/licenses/by/4.0/>).

1. Introduction

Time division multiple access (TDMA) achieves the effect of multi-user sharing communication resources by dividing a non-overlapping slot in time. TDMA has the advantages of large communication capacity, high frequency efficiency and compatibility between prime station and slave station. It has been widely used in various civil and military communication systems, such as very small aperture terminal (VSAT) satellite systems, international maritime satellite systems, iridium satellite systems and unmanned aerial vehicle communication systems [1–4]. TDMA signal usually has the characteristics of burst and transient. Detection of burst start time is important for subsequent parameter estimation and demodulation.

Since relative movement between the transmitter and receiver results in doppler frequency shift to receiving signals [5], distributed unique word (DUW) shows significant robustness for frequency shift, and it can achieve high precision frequency estimation in the subsequent frequency offset correction work. At present, many VSAT satellite burst communications use DUW instead of the traditional centralized UW. Therefore, the DUW detection method has practical application value for the burst signal using only DUW. In particular, under the background of wide use of high gain channel coding and miniaturization of sending terminal, the TDMA signal detection algorithm needs to work reliably at low SNR. This puts forward much stricter requirements for DUW detection. Therefore, DUW detection methods with high precision and robustness show great theoretical significance and application prospects.

1.1. Related Work

At present, there are mainly the following burst detection algorithms for TDMA signal. The energy based detection algorithm [6–8] can determine the existence of burst signal by detecting the energy within the window. This kind of method has good anti-frequency offset performance; however, it is sensitive to noise and is not suitable for detection under low SNR conditions. The frequency domain based detection method [9,10] leverages the frequency domain features of signal to detect the start position of burst signal. This method has good anti-noise performance; unfortunately, the realization complexity is impractical. The unique word (UW) based detection algorithm [11–13] can achieve high accuracy by detecting the burst of received signal through the self-correlation property of UW in the TDMA signal under the assumption that the receiver has the perfect prior knowledge of UW. However, current signal detection algorithms based on UW mainly consider the distribution of UW in signal frame head [14–17], and we have not seen much research on DUW, except Hou₁ and Hou₂ algorithms [18]. They have advantages of good anti-frequency offset, but do not behave well at lower SNR and are greatly influenced by the structure of UW. To sum up, in order to improve detection accuracy and robustness, burst detection based on DUW needs further research.

1.2. Our Contribution

In this paper, we propose a burst detection algorithm for DUW TDMA signals in satellite communications. The main contributions of this paper are shown in the following:

- (1) We analyze the principle of eliminating frequency offset and phase offset by traditional dual correlation (TDC) detection algorithm, which detects centralized UW, and apply it to DUW detection.
- (2) We analyze that DUW naturally has two different kinds of time delays, namely the delay within the group and the delay between the two groups. We combine them with TDC and propose a DUW dual correlation detection algorithm (the “DUWDC” described below). In addition, its advantage is that the change of DUW distribution structure will not affect its detection performance.
- (3) We carry out massive experiments to see the effects of frequency offset, signal to noise ratio, different distribution structures of DUW on detection performance. Simulation results show that DUWDC has good stability, high detection accuracy and good anti-frequency offset performance.

The rest of this article is arranged as follows: Section 2 is the system model, Section 3 is the algorithm description and Section 4 is the performance analysis. Section 5 is the simulation experiments and Section 6 is the conclusion.

2. System Model

In TDMA communication, MPSK modulation is often used. The received signal model after down-conversion is as follows:

$$r(k) = s(k)e^{j(\omega_0 kT + \theta)} + n(k) \quad (1)$$

Herein, $s(k) = e^{j\varphi(k)}$ is complex base-band signal, the value of $\varphi(k)$ is $2\pi q/M$, ($q = 0, 1, 2, \dots, M - 1$), T is symbol period, ω_0 is frequency offset, θ is phase offset, $n(k)$ is additive white gaussian noise (AWGN).

TDMA burst signals usually contain site identification code, UW, carrier and bit timing recovery code, instruction signal and information data. Since UW is not easily replicated by random data, it does not cause false detection and is used as a TDMA burst time base [19]. UW of traditional TDMA burst signal is generally continuous and concentrated in the start part of burst data, and its frame structure is shown in Figure 1.

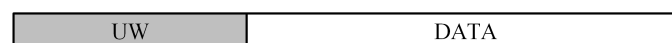


Figure 1. Traditional TDMA frame structure.

At present, a class of single carrier TDMA signals with new type DUW structure appears in satellite communication. The frame structure is shown in Figure 2. There are P groups of UW, and each group of UW has N symbols. It is inserted into the burst signal at equal intervals with L_0 symbols as a period. In one burst signal, the total length of UW is $D = N \times P$ symbols.

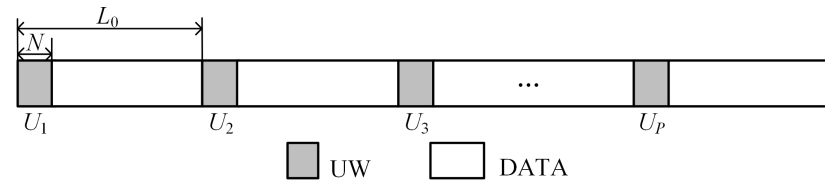


Figure 2. Distributed unique word TDMA frame structure.

As shown in Figure 3, the known local UW sequence $a(k)$ is composed of the above U_1 to U_P groups arranged in series.

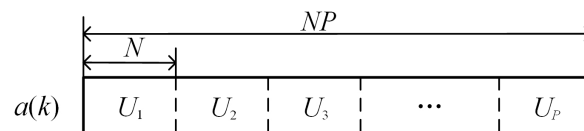


Figure 3. The known local UW structure.

The expression of $a(k)$ is:

$$a(k) = a(iN + j) = e^{j\phi(i,j)}, \quad i = 0, 1, \dots, P - 1, \quad (2)$$

$$j = 0, 1, \dots, N - 1, \quad k = iN + j$$

Herein, $e^{j\phi(i,j)}$ represents the j -th UW symbol in the i -th group, and its position in sequence $a(k)$ is shown by $k = iN + j$.

3. Algorithm Description

3.1. Traditional Centralized Dual Correlation Detection Algorithm

TDC detection algorithm [20,21] is mainly based on centralized UW to detect and synchronize burst signals. The detection principle is shown in Figure 4.

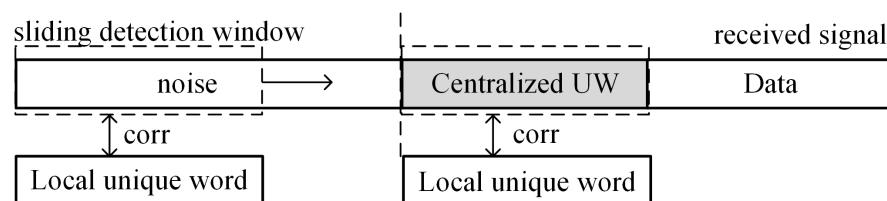


Figure 4. TDC detection principle.

As shown in Figure 4, the sliding detection window is concentrated and continuous in TDC detection algorithm. So, the signal selected by this window is continuous in waveform and frequency offset.

TDC detection formula[21] based on burst signal is:

$$L = \sum_{d=1}^{D-1} \left\{ \frac{\left| \sum_{k=d}^{D-1} r^*(k)a(k)r(k-d)a^*(k-d) \right|^2}{\sum_{k=d}^{D-1} |r^*(k)r^*(k-d)|^2} \right\} \quad (3)$$

Herein, D is the total length of UW, L is correlation coefficient, $*$ in x^* is complex conjugate.

The numerator in Equation (3) can be written as:

$$corr = \left| \sum_{k=d}^{D-1} r^*(k)r(k-d) \{a^*(k)a(k-d)\}^* \right|^2 \tag{4}$$

Equation (4) is the core of dual correlation algorithm. Bring Equation (1) into Equation (4), for the convenience of discussion, let $d = 1$, consider the non-correlation between noise and UW, ignore the influence of noise, we can obtain:

$$\begin{aligned} corr &= \left| \sum_{k=1}^{D-1} r^*(k)r(k-1) \{a^*(k)a(k-1)\}^* \right|^2 \\ &= \left| \sum_{k=1}^{D-1} s^*(k)s(k-1) \{a^*(k)a(k-1)\}^* e^{-j\omega_0 T} \right|^2 \end{aligned} \tag{5}$$

Since the signal in sliding detection window is continuous on frequency offset, the delay conjugate multiplication $r^*(k)r(k-1)$ in Equation (5) converts the frequency offset to one fixed phase offset $e^{-j\omega_0 T}$. Then this phase offset is eliminated by the modulo operation, and when the sliding detection window is aligned with the UW of received signal, $s(k) = a(k)$ for any k , then $s^*(k)s(k-1) \{a^*(k)a(k-1)\}^* = 1$, $corr$ will be maximum.

3.2. DUWDC Detection Algorithm

As shown in Figure 2, DUW is uniformly dispersed in a burst signal, and we allocated the sliding detection windows with the same structures as DUW. As shown in Figure 5, sliding detection window has a total of P groups, and there are L_0 symbols between the adjacent two groups, with N symbols for each group length. Sequence $r_0(k)$ is composed of the received data selected by the sliding detection window.

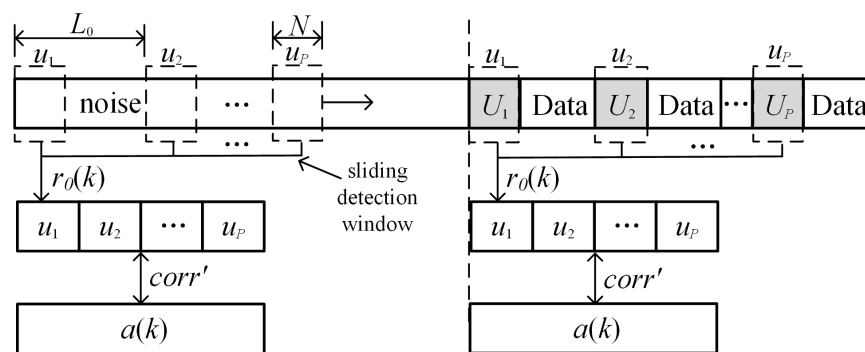


Figure 5. DUW burst signal detection principle.

As shown in Figure 5, sequence $r_0(k)$ is composed of P discrete receiving data groups, its waveform and frequency offset are discontinuous. As shown in Figure 6, the symbols within each group are continuous, while actual distance between the two symbols at the adjacent group connection part is $L_0 + 1 - N$ symbol.

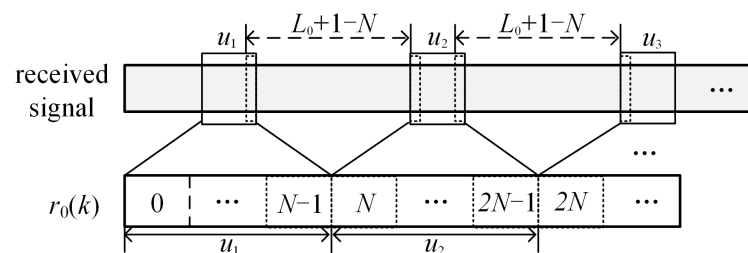


Figure 6. The discontinuity of $r_0(k)$.

The expression of $r_0(k)$ is:

$$\begin{aligned}
 r_0(k) &= r_0(iN + j) \\
 &= r(iL_0 + j), \quad i = 0, 1, \dots, P - 1, \\
 & \quad j = 0, 1, \dots, N - 1, \quad k = iN + j
 \end{aligned}
 \tag{6}$$

As described in Section 3.1, $r^*(k)r(k - 1)$ can convert the frequency offset to one fixed phase offset, so it can be eliminated by one modulo operation. However, as shown in Figure 7, $r_0^*(k)r_0(k - 1)$ contains two different kinds of time delays, namely one symbol and $L_0 + 1 - N$ symbols. In addition, it will convert the frequency offset to two different fixed phase offsets, namely $e^{-j\omega_0 T}$ and $e^{-j(L_0+1-N)\omega_0 T}$. So, they cannot be eliminated by one modulo operation.

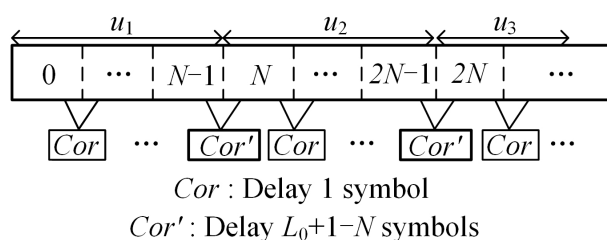


Figure 7. Two different kinds of time delays in $r_0^*(k)r_0(k - 1)$.

Therefore, based on the delay within the group and the delay between the two groups, we divide the dual correlation formula into two parts to calculate the modulus separately, that is:

$$\begin{aligned}
 corr' &= \left| \sum_{i=0}^{P-1} \sum_{k=iN+1}^{(i+1)N-1} r_0^*(k)r_0(k - 1) \{a^*(k)a(k - 1)\}^* \right| \\
 &+ \left| \sum_{i=1}^{P-1} r_0^*(iN)r_0(iN - 1) \{a^*(iN)a(iN - 1)\}^* \right|
 \end{aligned}
 \tag{7}$$

Herein, the first part is the dual correlation between symbols within each group, and the second part is the dual correlation between symbols in the adjacent group connection part.

Bring Equations (1) and (6) into Equation (7), consider the non-correlation between noise and UW, and ignore influence of noise, Equation (7) can be rewritten as follows:

$$\begin{aligned}
 corr' &= \left| \sum_{i=0}^{P-1} \sum_{k=iN+1}^{(i+1)N-1} s^*(k)s(k - 1) \{a^*(k)a(k - 1)\}^* e^{-j\omega_0 T} \right| \\
 &+ \left| \sum_{i=1}^{P-1} s^*(iN)s(iN - 1) \{a^*(iN)a(iN - 1)\}^* e^{-j(L_0+1-N)\omega_0 T} \right|
 \end{aligned}
 \tag{8}$$

As shown in Equation (8), the frequency offset is converted to two different fixed phase, and fixed phase is eliminated by two modulo operation. Then the sliding detection window is aligned with the UW of received signal, and $corr'$ will be maximum.

3.3. Algorithm Step

Let $b(k) = \sum_{k=1}^{NP-1} a^*(k)a(k - 1)$, because $a(k)$ is a known sequence, $b(k)$ can be computed locally in advance, and Equation (7) can be simplified to the following form:

$$\begin{aligned}
 corr' &= \left| \sum_{i=0}^{P-1} \sum_{k=iN+1}^{(i+1)N-1} r_0^*(k)r_0(k - 1)b^*(k) \right| \\
 &+ \left| \sum_{i=1}^{P-1} r_0^*(iN)r_0(iN - 1)b^*(iN) \right|
 \end{aligned}
 \tag{9}$$

The steps of DUWDC are as follows:

- (1) Sliding detection window with distributed structure extracts sequence $r_0(k)$ from receiving single;

- (2) Bring $r_0(k)$ into Equation (9) to obtain correlation coefficient;
- (3) Slide the detection window back and extract the sequence $r_0(k)$ again;
- (4) Repeat step 2 to step 3 until correlation coefficient of the whole data is obtained, and threshold detection output burst start position.

4. Performance Analysis

4.1. Robustness Analysis

From Equations (7) and (8), it can be seen that the frequency offset is converted to fixed phase offset $e^{j\omega_0 T}$ and $e^{j(L_0+1-N)\omega_0 T}$ by DUWDC algorithm, and two phase offsets are eliminated by modular operation, respectively, which will not affect correlation results. It shows that DUWDC inherits anti-frequency offset performance of TDC algorithm perfectly.

Hou₁ and Hou₂ are the existing DUW detection algorithms, and their algorithm formula is as follows:

$$corr_{Hou_1} = \left| \sum_{i=0}^{p-1} \sum_{k=iN+1}^{(i+1)N-1} r_0^*(k)r_0(k-1)\{a^*(k)a(k-1)\}^* \right| \tag{10}$$

$$corr_{Hou_2} = \left| \sum_{i=1}^{p-1} \sum_{k=iN}^{(i+1)N-1} r_0^*(k)r_0(k-N)\{a^*(k)a(k-N)\}^* \right| \tag{11}$$

It can be seen from Equations (10) and (11) that Hou₁ and Hou₂ both use similar dual correlation algorithm, but their delay rules are different from the algorithm in this paper. The number of points involved in the correlation operation between receiving sequence and local sequence is also different, and of Hou₁ and Hou₂ it is $(N - 1)P$ and $(P - 1)N$, respectively. It can be seen from Equation (7) that the number of points involved in the correlation operation of DUWDC is $N \times P - 1$. N and P depend on the distribution structure of DUW. When the ratio of N and P changes, the number of correlation operation points of DUWDC remains the same, but of Hou₁ and Hou₂ it is variable, as shown in Figure 8. This is where we assume that the total length of DUW is 48 symbols ($N \times P = 48$), and N is equal to 2, 4, 6, 12 and 16, respectively.

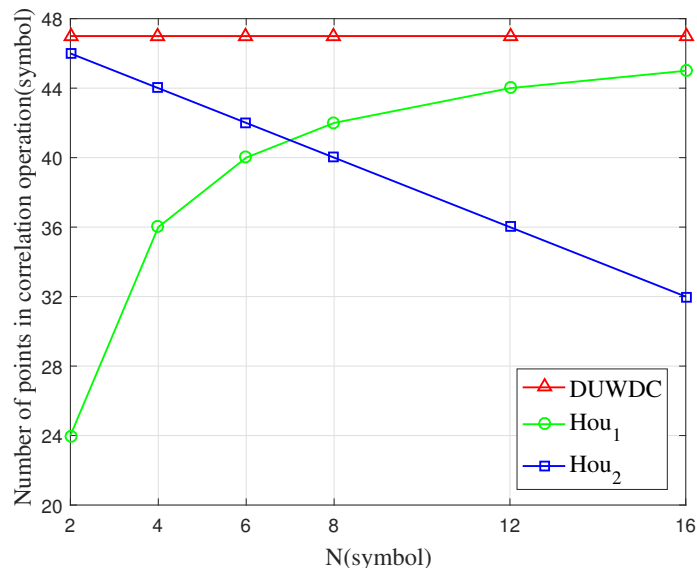


Figure 8. The relationship between the number of correlation operation points and UW distribution structure.

Generally, the longer the sequence involved in the correlation operation is, the better the correlation effect [18]. Therefore, the advantage of DUWDC over Hou₁ and Hou₂ is that the change of UW distributed structure cannot affect detection performance, and the number of points involved in correlation operation has been maximized, and correlation effect is better.

4.2. Complexity Analysis

Taking complex multiplication and complex addition required for each correlation coefficient calculation as examples, complexity of different detection algorithms is compared, as shown in Table 1.

Table 1. Complexity comparison of four detection algorithms.

Algorithm	Multiplication	Addition
Traditional dual correlation [21]	$(NP - 1)NP$	$0.5(NP - 1)NP$
Hou ₁	$2(N - 1)P$	$(N - 1)P$
Hou ₂	$2(P - 1)N$	$(P - 1)N$
DUWDC	$2(NP - 1)$	$NP - 1$

It can be seen from Table 1 that the complexity of DUWDC is lower than the traditional dual correlation detection algorithm, and its multiplication and addition times are both $\frac{2}{N \times P}$ of the latter, where $N \times P = D$ is the total number of DUW symbols, generally far greater than two. Compared to Hou₁ and Hou₂, the complexity of DUWDC is slightly improved, its multiplication times are $\frac{D-1}{D-P}$ and $\frac{D-1}{D-N}$ of Hou₁ and Hou₂, respectively, and the same is true for addition.

5. Simulation Experiments

In order to verify the proposed algorithm, simulation signal is tested in the MATLAB environment. Assume that signal modulation mode is QPSK, symbol rate R_s is 2 MBaud, sampling rate F_s is 8 MHz, sampling time is 25 ms, there are three TDMA burst signals, each burst time is 0.36 ms.

Firstly, in order to test the influence of frequency offset on the detection effect of DUWDC, channel environment is assumed to be additive Gaussian white noise, $E_b/N_0 = \{0 \text{ dB}, 3 \text{ dB}, 6 \text{ dB}, 9 \text{ dB}\}$, the total number of UW is 48 symbols and UW distribution structure: $N = 2$; $P = 24$; $L_0 = 100$. The signals with normalized frequency offset $f_e T = 0$ and $f_e T = 0.1$ are detected, respectively.

The correlation coefficient curves obtained under different frequency offsets are shown in Figures 9 and 10. In the case of two normalized frequency offsets, detection effect of DUWDC is basically the same, indicating that it has good anti-frequency offset performance and can be used in large frequency offset environments. The analysis of anti-frequency offset performance of the algorithm is verified.

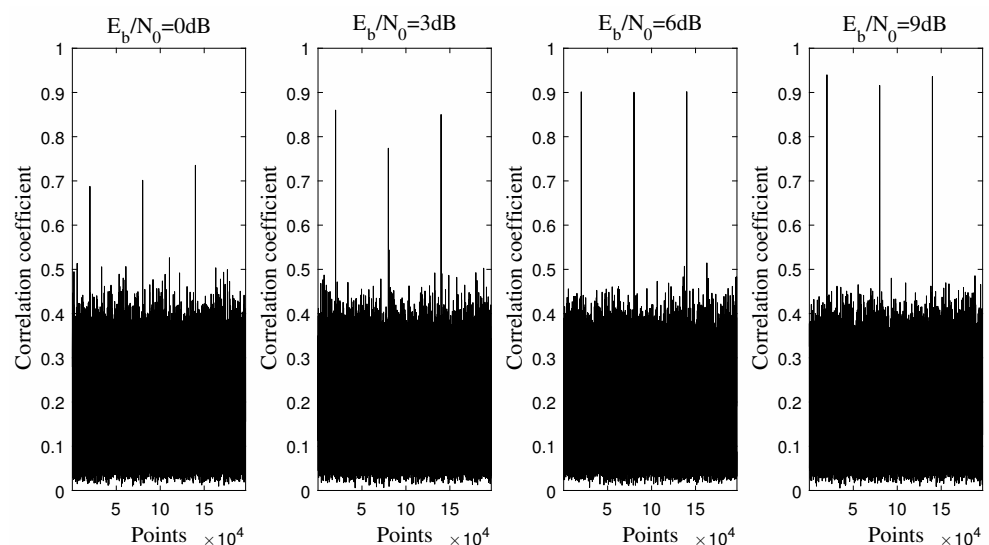


Figure 9. The correlation coefficient curves obtained by DUWDC in the case of $f_e T = 0$.

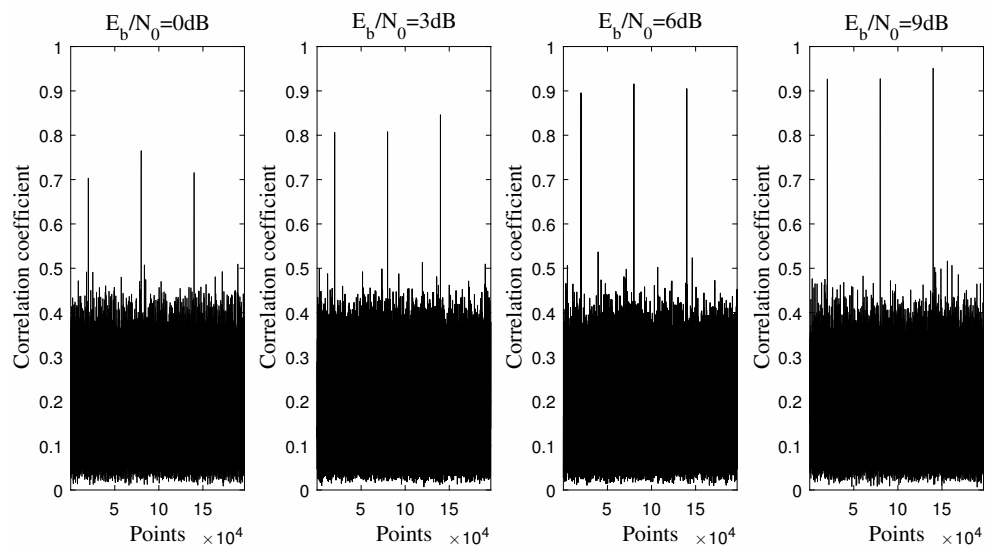


Figure 10. The correlation coefficient curves obtained by DUWDC in the case of $f_eT = 0.1$.

In order to verify the influence of DUW distribution structure on the algorithm performance, simulation conditions: let $E_b/N_0 = 6$ dB, normalized frequency offset $f_eT = 0.1$, the total number of UW is 48 symbols and the number of symbols inserted in each group is 2, 4, 8 and 16, respectively. As shown in Figure 11, under different distribution structures, detection results are basically the same. Qualitatively verify the theoretical analysis that detection performance of DUWDC is not affected by the distributed structure.

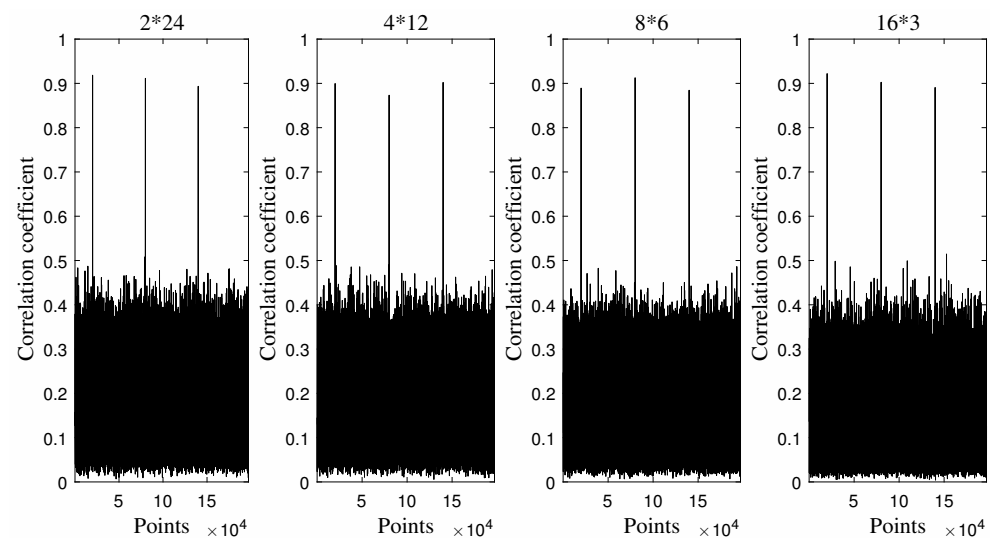


Figure 11. The correlation coefficient curves obtained by DUWDC under different DUW distribution structures.

Based on the above analysis and simulation results, DUWDC has good anti-frequency offset performance, and detection performance increases with the increase in SNR. It is not affected by UW distribution structure and has good robustness to different distribution structures.

For influence of different SNR on the false alarm probability of DUWDC, Monte Carlo simulation is performed on the algorithm under the condition of normalized frequency offset $f_eT = 0.1$. As shown in Figure 12, let $E_b/N_0 = \{-3$ dB, 0 dB, 3 dB, 6 dB, 9 dB $\}$, false alarm probability of algorithm under different thresholds th is counted, respectively.

In the oversampling rate $F_s/R_s = 4$ in the experiment, actual correlation results generally have two to four positions, which can be judged as the start of burst signal, then

select one of the largest correlation coefficient positions to judge the accurate position. From Figure 12, it can be seen that the larger correlation threshold and the higher SNR, the smaller false alarm probability, and the false alarm of DUWDC algorithm changes little with SNR.

In order to further verify detection performance of DUWDC, based on DUW TDMA signal, DUWDC, Hou₁ and Hou₂ are simulated and compared. Simulation conditions: normalized frequency offset $f_e T = 0.1$, $E_b/N_0 = \{-3 \text{ dB}, 0 \text{ dB}, 3 \text{ dB}, 6 \text{ dB}\}$, the total number of UW is 48 symbols and DUW structure: $N = 2$; $P = 24$; $L_0 = 100$. Monte Carlo experiments are carried out on this signal. Under the threshold of false alarm probability $P_f < 10^{-5}$, detection probabilities P_d of each algorithm under different E_b/N_0 are counted, respectively.

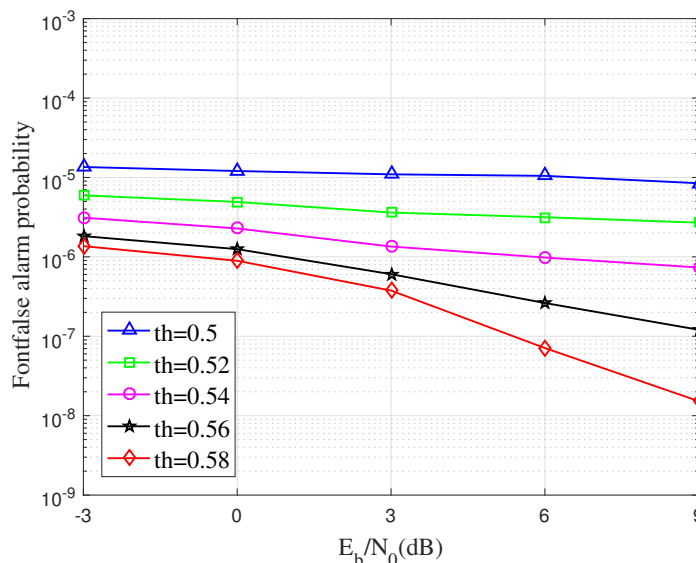


Figure 12. False alarm probability of DUWDC under different SNR.

Compared with Hou₁ and Hou₂, DUWDC has more points involved in related operations and better detection performance. It can be seen from Figure 13 that when E_b/N_0 is at -3 dB to 1 dB , DUWDC performance is about 0.8 dB better than Hou₂ under the same detection probability.

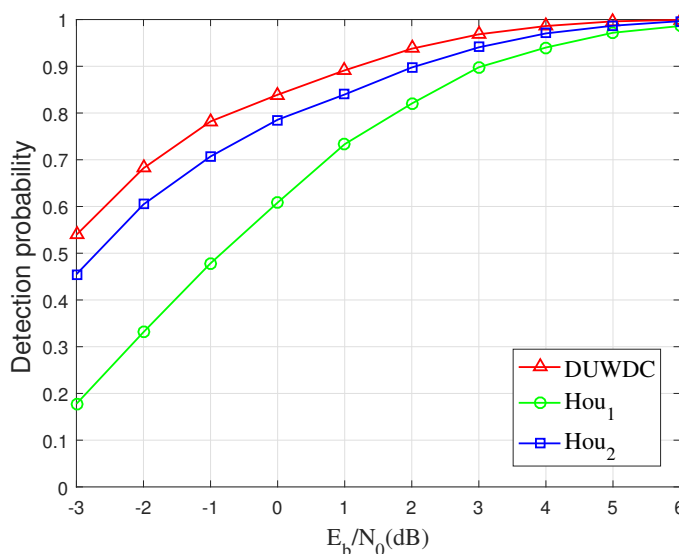


Figure 13. Relationship curve between the detection probability and SNR.

At the same time, in order to better compare the detection performance of DUWDC under high E_b/N_0 , Figure 14 gives the relationship curve between the missed detection probability and E_b/N_0 . It can be seen that the missed detection probability of DUWDC is significantly lower than that of Hou₁ and Hou₂. In addition, when E_b/N_0 is at 1 dB to 6 dB, DUWDC performance is about 1 dB better than Hou₂ under the same missed detection probability.

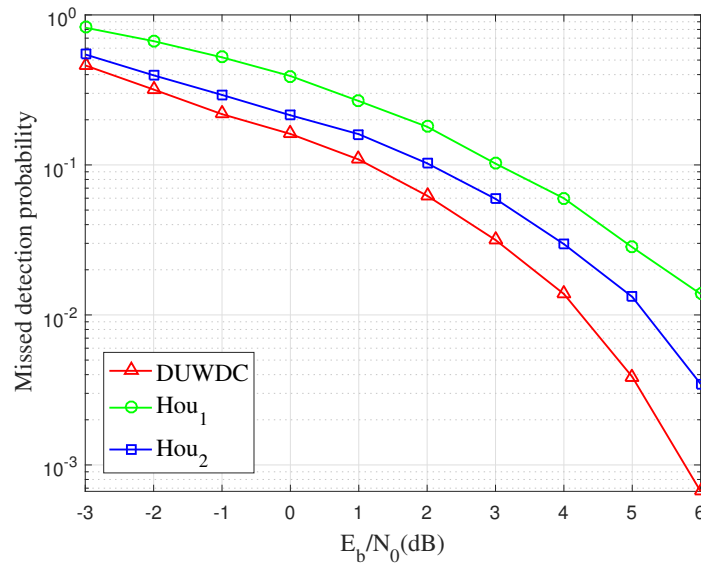


Figure 14. Relationship curve between the missed detection probability and SNR.

To verify the robustness of the algorithm, based on DUW TDMA signal, DUWDC, Hou₁ and Hou₂ are simulated and compared. Simulation conditions: normalized frequency offset $f_e T = 0.1$, $E_b/N_0 = -1$ dB, the total number of UW is 48 symbols and the number of symbols inserted in each group is 2, 4, 6, 8, 12 and 16. Monte Carlo experiments are carried out on this signal. Under the threshold of false alarm probability $P_f < 10^{-5}$, the detection probabilities P_d of each algorithm under different UW distribution structures are counted, respectively. The experimental results are shown in Figure 15.

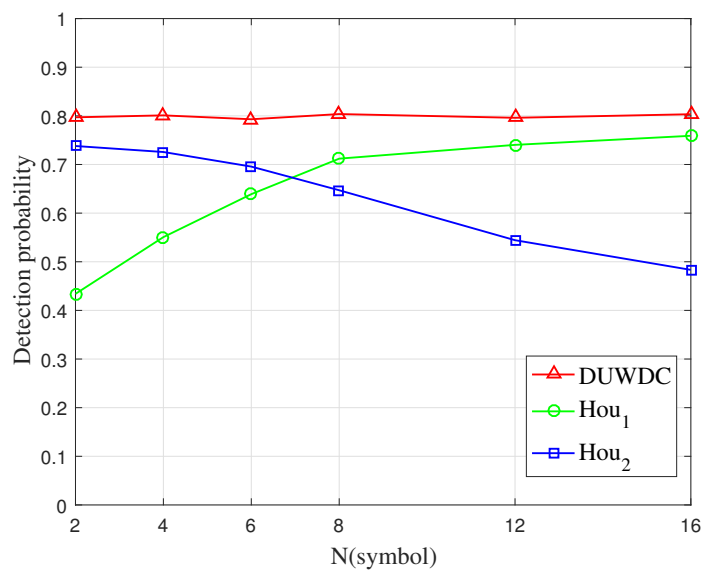


Figure 15. Influence of different UW distribution structures on algorithm detection performance.

It can be seen from Figure 15 that under the same SNR, detection probability of DUWDC is at the same level for DUWs with different distribution structures, while of

Hou₁ and Hou₂ it fluctuates greatly. $\frac{1}{n} \sum_{i=1}^n (x_i - x)^2$ is used to calculate the variance of the curves in the figure; Hou₁ and Hou₂ are 0.0133 and 0.009, respectively, and DUWDC is 1.56×10^{-5} , which is 99.83% lower than Hou₂. This shows that DUWDC has good stability. The analysis of robustness of the algorithm in Section 4.1 is verified quantitatively.

6. Conclusions

In this paper, a robust burst detection algorithm for distributed unique word (DUW) TDMA signal is proposed. First of all, we analyze the principle of traditional dual correlation (TDC) and the influence of DUW structure on the delay conjugate multiplication. We combine DUW with TDC and obtain a dual correlation detection algorithm, which is suitable for DUW. The experimental results show that the proposed algorithm has high detection accuracy and good stability. Under the same SNR, detection probability of the algorithm is at the same level for DUWs with different distribution structures. In addition, when the normalized frequency offset is 10% and SNR is greater than 4dB, detection probability of the algorithm is greater than 98%, which is better than the existing DUW detection algorithms.

Author Contributions: Conceptualization, K.Z. and J.D.; methodology, K.Z., K.G. and Z.L.; software, K.Z.; validation, K.Z., K.G. and J.D.; writing—original draft preparation, K.Z.; writing—review and editing, K.Z., P.S. and J.D.; project administration, J.D., K.G. and P.S. All authors have read and agreed to the published version of the manuscript.

Funding: This research was funded by the National Natural Science Foundation of China (No. 61901417), the Science and Technology Key Project of Henan Province (No. 212102210173 and No. 212102210566), the Cutting-edge Science and Technology Innovation Project of the Key Research and Development Program of China (No. 2019QY0302).

Institutional Review Board Statement: Not applicable.

Informed Consent Statement: Not applicable.

Data Availability Statement: The data presented in this study are available on request from the corresponding author.

Acknowledgments: We sincerely thank the members of the Communication Signal Analysis and Countermeasure Laboratory of the School of Information Engineering of Zhengzhou University.

Conflicts of Interest: The authors declare no conflict of interest.

References

1. Shin, M.-S.; Ryu, J.-G.; Oh, D.-G. On the network clock reference variation compensation for satellite tdma network. In Proceedings of the 2017 International Conference on Information and Communication Technology Convergence (ICTC), Jeju, Korea, 18–20 October 2017; pp. 1216–1218.
2. Zheng, B.; Yen, K.; Peng, X.; Zhang, R. Angle partition-based tdma for vdes satellite multiuser downlink communications. In Proceedings of the GLOBECOM 2020—2020 IEEE Global Communications Conference, Taipei, Taiwan, 7–11 December 2020; pp. 1–6.
3. Zhu, J.; Cheng, J.; Tian, Y.; Wang, Y.; Chang, J. A method of system timing in tdma systems for leo satellites. In Proceedings of the 2019 IEEE 2nd International Conference on Electronic Information and Communication Technology (ICEICT), Harbin, China, 20–22 January 2019; pp. 113–117.
4. Cheon, H.-R.; Cho, J.-W.; Kim, J.-H. Dynamic resource allocation algorithm of uas by network environment and data requirement. In Proceedings of the 2017 International Conference on Information and Communication Technology Convergence (ICTC), Jeju, Korea, 18–20 October 2017; pp. 383–387.
5. Wei, Q.; Chen, X.; Zhan, Y.F. Exploring implicit pilots for precise estimation of leo satellite downlink doppler frequency. *IEEE Commun. Lett.* **2020**, *24*, 2270–2274. [[CrossRef](#)]
6. Urkowitz, H. Energy detection of unknown deterministic signals. *Proc. IEEE*, **1967**, *55*, 523–531. [[CrossRef](#)]
7. Chen, Y. Improved energy detector for random signals in gaussian noise. *IEEE Trans. Wirel. Commun.* **2010**, *9*, 558–563. [[CrossRef](#)]
8. Oh, H.; Nam, H. Energy detection scheme in the presence of burst signals. *IEEE Signal Process. Lett.* **2019**, *26*, 582–586. [[CrossRef](#)]
9. Wang, Q.; Xie, Z.; Hu, J.; Zhang, G. Blind detection of satellite communication signals based on cyclic spectrum. In Proceedings of the 2015 International Conference on Wireless Communications Signal Processing (WCSP), Nanjing, China, 15–17 October 2015; pp. 1–5.

10. Li, S.; Yan, K.; Xiong, H. Efficient feature extraction of cycle spectrum and weak communication signal detection. In Proceedings of the 2017 IEEE/CIC International Conference on Communications in China (ICCC), Qingdao, China, 22–24 October 2017; pp. 1–6.
11. Zhang, J.; Xiang, J.; Zhu, Z. The detection of unique word at lower snr. *J. Electron. Inf. Technol.* **2001**, *23*, 1116–1122.
12. Pedone, R.; Villanti, M.; Vanelli-Coralli, A.; Corazza, G.E.; Mathiopoulos, P.T. Frame synchronization in frequency uncertainty. *IEEE Trans. Commun.* **2010**, *58*, 1235–1246. [[CrossRef](#)]
13. Ying, W.; Liu, X.; Chen, Z.; Liu, J.; Wang, H.; Cheng, G. A modified frame synchronization algorithm based on average likelihood ratio testing. In Proceedings of the 2020 15th IEEE International Conference on Signal Processing (ICSP), Beijing, China, 6–9 December 2020; Volume 1, pp. 417–422.
14. Xu, L.; Chen, X.; Chen, Y.; Liu, K. Simulation research on phase modulation signal detection in satellite communication. *Comput. Simul.* **2018**, *35*, 191–194.
15. Peng, Y.; Sun, C.; Zhang, T. Tdma burst detection method based on unique code symbol distance. *J. Shanghai Univ. Electr. Power* **2020**, *36*, 391–394.
16. Liu, Z.; Gong, K.; Sun, P.; Deng, J.; Zou, K.; Duan, L. Oqpsk synchronization parameter estimation based on burst signal detection. *Electronics* **2021**, *10*, 69. [[CrossRef](#)]
17. He, Z.; Sun, P.; Gong, K.; Jiang, H. Parameter estimation and signal detection algorithm based on adaptive capture in non-cooperative communication. *MATEC Web Conf.* **2021**, *336*, 13. [[CrossRef](#)]
18. Hou, X.; Li, T.; Yang, S. Detection and frequency estimation of distributed unique word tdma signal. *Signal Process.* **2018**, *30*, 1211–1220.
19. Ippolito, L.J. *Satellite Communications Systems Engineering: Atmospheric Effects, Satellite Link Design and System Performance*; John Wiley & Sons: Hoboken, NJ, USA, 2017.
20. Choi, Z.Y.; Lee, Y. Frame synchronization in the presence of frequency offset. *IEEE Trans. Commun.* **2002**, *50*, 1062–1065. [[CrossRef](#)]
21. Huang, Y.; Lu, Y.; Yuan, Q. Robust burst detection based on the average likelihood ratio test. *J. Electron. Inf. Technol.* **2010**, *32*, 345–349. [[CrossRef](#)]